17th World Conference on Earthquake Engineering, 17WCEE
Sendai, Japan - September 13th to 18th 2020

CONTRIBUTION OF THE GRAVITY BEAM-COLUMN CONNECTIONS TO THE SEISMIC RESERVE CAPACITY OF STEEL BUILDINGS

T. Béland[(1)], R. Tremblay[(2)], L. A. Fahnestock[(3)], E. M. Hines[(4)]

[(1)] *Ph.D candidate, Polytechnique Montréal, Montreal, QCH3C 3A7, Canada, thierry.beland@polymtl.ca*
[(2)] *Professor, Polytechnique Montréal, Montreal, QC H3C 3A7, Canada, robert.tremblay@polymtl.ca*
[(3)] *Professor, University of Illinois at Urbana-Champaign, Urbana, Illinois 61801, USA, fhnstck@illinois.edu*
[(4)] *Professor, Tufts University, Medford, Massachusetts, 02155, USA, eric.hines@tufts.edu*

Abstract

To increase the seismic robustness of steel buildings, partially restrained (PR) connections can be implemented between beams and columns of the building gravity framing system. These connections create a moment-frame action in the gravity frames that can increase significantly the lateral reserve capacity of the structure. This behaviour may be beneficial to mitigate P-delta effects and increase the collapse prevention capacity of the building, especially in low-ductility buildings where yielding hierarchy is not well defined. Top and seat angles acting together with double web clip angles form an economically viable option to obtain PR connections exhibiting strength and ductility. To accurately represent the hysteretic behaviour of the gravity connections, a model developed with a component-based approach is presented and validated with the hysteretic behaviour of full-scale beam-column subassemblies characterized experimentally. This numerical model is then integrated in a complete model of a typical low-ductility building using the OpenSees finite element analysis software. The same building is modelled with pinned beam-column connections under the same loading conditions to serve as a comparative basis. The seismic response of both buildings is presented in detail and the contribution of the gravity beam-column connections in the reserve capacity is assessed. The reserve capacity created by these gravity frame connections contributed to maintaining the seismic response within acceptable limits after failure of a first-storey brace connection. Compared to a building with pinned gravity frame connections, storey drifts and column moments were reduced, confirming the potential for PR connections to decrease the risk of soft storey response and structural collapse.

Keywords: Steel Buildings; Reserve capacity; Beam-column connections; Top and seat angles.

1. Introduction

In low and moderate seismic regions of North America, it is permitted to use steel seismic force resisting systems (SFRSs) that are not specifically designed and detailed to achieve ductile seismic response [1,2]. These structures are considered as low ductility systems since the energy dissipation is essentially assumed to be provided by the inherent ductility of steel and friction at connection interfaces. In Canada, these structures fall in the Conventional Construction (Type CC) category, for which ductility- and overstrength-related force modification factors R_d = 1.5 and R_o = 1.3 are specified. Type CC steel SFRSs in buildings up to 15 m can be designed solely with the non-seismic provisions of the CSA S16 steel design standard [3]. However, to avoid brittle failure of connections along the lateral load path, seismic induced forces must be increased by 1.5 for connection design in higher seismic regions unless the governing limit states for the connection are ductile. Type CC SFRSs may also be adopted for structures taller than 15 m, granted an increase of the seismic design loads as a function of the height and additional design and detailing requirements. In practice, Type CC category is the preferred choice for a large portion of low-rise steel buildings because it avoids the complexities of capacity design and special detailing and design requirements that are prescribed for all other steel SFRSs. However, the building response is not well evaluated during the design since no specific yielding hierarchy is prescribed. In this context, there is a strong motivation for better understanding the seismic behaviour of Type CC buildings.

Recent studies have shown that earthquake robustness of steel SFRSs can be significantly enhanced by means of the reserve lateral capacity provided by partially-restrained (PR) beam-column joints in the building gravity load resisting system [4-6]. Adding top and seat angles to simple double web clip angles beam-column connections can form an economically viable option to increase the connection flexural strength and ductility. Several past experimental programs have been conducted on this connection type to characterize the nonlinear behaviour of their components under rotational demand [7-9]. However, limited study had been performed to assess the benefit and contribution to the reserve lateral capacity of steel buildings. A joint U.S.-Canada research project was therefore undertaken to investigate the seismic response of low-ductility systems with PR connections implemented in the gravity system. The project included an experimental program to characterize the influence of geometrical parameters of bolted angles on their strength, plastic deformation capacity, and hysteretic behaviour on a component level [10]. A second experimental program was conducted on full-scale bolted double web angle connections enhanced with top and seat angles subjected to both gravity shear loading and seismic rotational demand [11, 12]. Finally, effective numerical models were developed to reproduce the cyclic inelastic response of bolted angles on a component level [13].

This article presents a numerical study illustrating the beneficial effects of using partially restrained beam-column connections in the gravity system to prevent structural collapse. The prototype structure studied is a 3-storey Type CC braced frame structure with brace connections designed for seismic loads without the 1.5 amplification factor. In that case, the reserve system would be mobilized in the case of a brace connection failure. The prototype building is described first, together with the numerical model that was developed with the OpenSees finite element software [14] to investigate its seismic response. Proposed design requirements for the PR connections are briefly introduced and applied to the structure. A new PR connection model specifically developed to reproduce numerically the results obtained from the full-scale beam-column joint tests is then presented in detail. This numerical model has been integrated in the structure model to evaluate the contribution of reserve lateral capacity to structural collapse prevention. The results of the structure analysis performed without the PR connections are also presented for comparison purposes.

2. Building models

The 3-storey prototype building is shown in Fig. 1. Type CC chevron bracing is used to resist lateral loads in both directions. The structure was designed for Montreal, QC, assuming a site class C (firm ground), in accordance with the 2015 NBCC [1] and CSA S16-14 [3]. The influence of the reserve capacity is evaluated

by comparing the seismic response of the structure for two different conditions for the beam-column connections of the gravity frame. In the first case, the connections are modelled as pinned connections to represent simple shear double web angle connections, as typically done in the design of these buildings. In the second case, the gravity frame in the structure model includes the PR double web bolted angles connections enhanced with top and seat angles.

2.1 Building description and design

The structure consists of five 9144 mm wide bays in both directions and 3 storeys of 4572 mm in height. The slab is extended 300 mm on the perimeter of each floor. Beams and columns are ASTM A992 shapes (F_y = 345 MPa) whereas braces are ASTM A500, grade C, square tubing (F_y = 345 MPa).

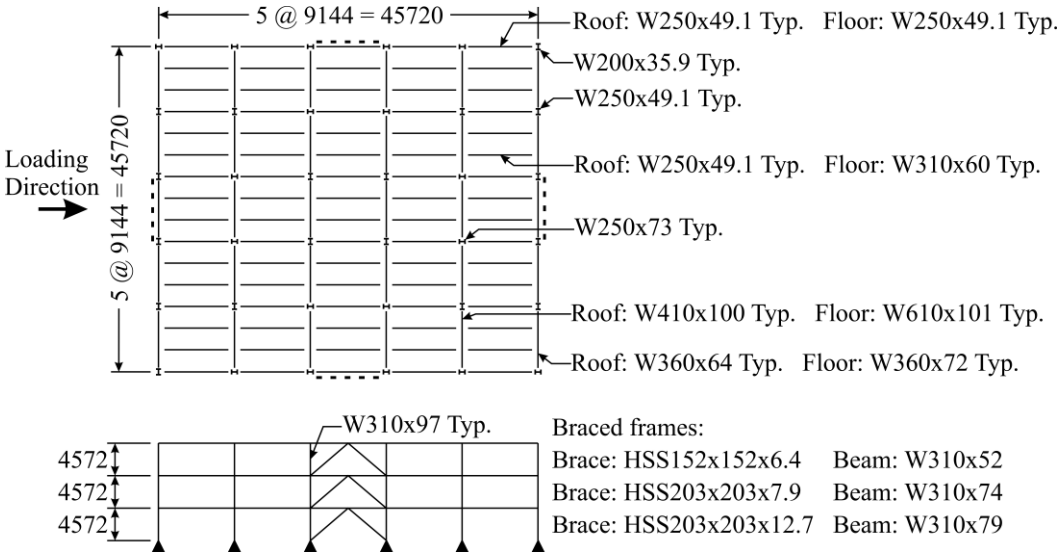

Fig. 1 – Building geometry and member sections

The design gravity loads at the roof level are: 1.2 kPa of dead load (D), 2.48 kPa of snow load (S) and 1.0 kPa of live load (L). At the floor levels, the gravity loads are: D = 3.5 kPa and L = 2.4 kPa. The floor dead load includes 1.0 kPa for partitions; this partition load is reduced to 0.5 kPa for the calculation of the floor seismic weight W_i, as permitted by NBCC. The seismic weights and total concomitant gravity loads (ΣP_i) at every level are given in Table 1. Concomitant gravity loads are determined for the combination 1.0D + 0.5L + 0.25S and are used in design and analysis to account for global P-Δ effects and P-δ effects on the column members. Gravity loads were determined individually for each column, including live load reduction permitted in NBCC. The total gravity loads in Table 1 correspond to the sum of the column loads for each storey.

The storey shears V_i and brace seismic forces $T_{f\text{-}E}$ or $C_{f\text{-}E}$ are also presented in Table 1. The seismic loads were determined using the NBCC equivalent static force procedure with force modification factors R_d of 1.5 and R_o of 1.3 The period T_a used to determine the seismic loads was 0.69 s, as determined with the NBCC empirical equation. The resulting base shear for the entire building was 2951 kN (0.128 W). Accidental in-plane torsion effects were included in the design of the braced frames. Each frame was thus designed for 60% of the total seismic loads. In chevron bracing, braces are selected to resist applied compressive loads. In the first storey, the brace design compressive loads due to gravity and seismic loads were 104 and 1282 kN, respectively, which resulted in a design factored load of 1386 kN for the brace connections. For this study, it was assumed that the brace connections would be designed for the same load. The same approach was used at all levels. The selected member sections are given in Fig. 1.

Table 1 – Seismic ang gravity loads of the studied building

Storey *i*	Seismic weight *W* (kN)	Storey shear V_i (kN)	Brace seismic force $T_{f\text{-}E}$, $C_{f\text{-}E}$ (kN)	Gravity loads ΣP_i (kN)
3	4410	952	404	4481
2	9592	2332	989	15271
1	9592	3022	1282	25970

2.2 Modelling of the frame members

Half of the example building structure was represented in the numerical model. The interior gravity frames were included in parallel to the braced frame, as pictured in Fig. 2a. The lateral displacement of the braced frame was linked to the interior frames with horizontal joint constraints (*EqualDOF*) at each storey. Concomitant gravity loads were applied on each column to account for global and member stability effects in the analysis.

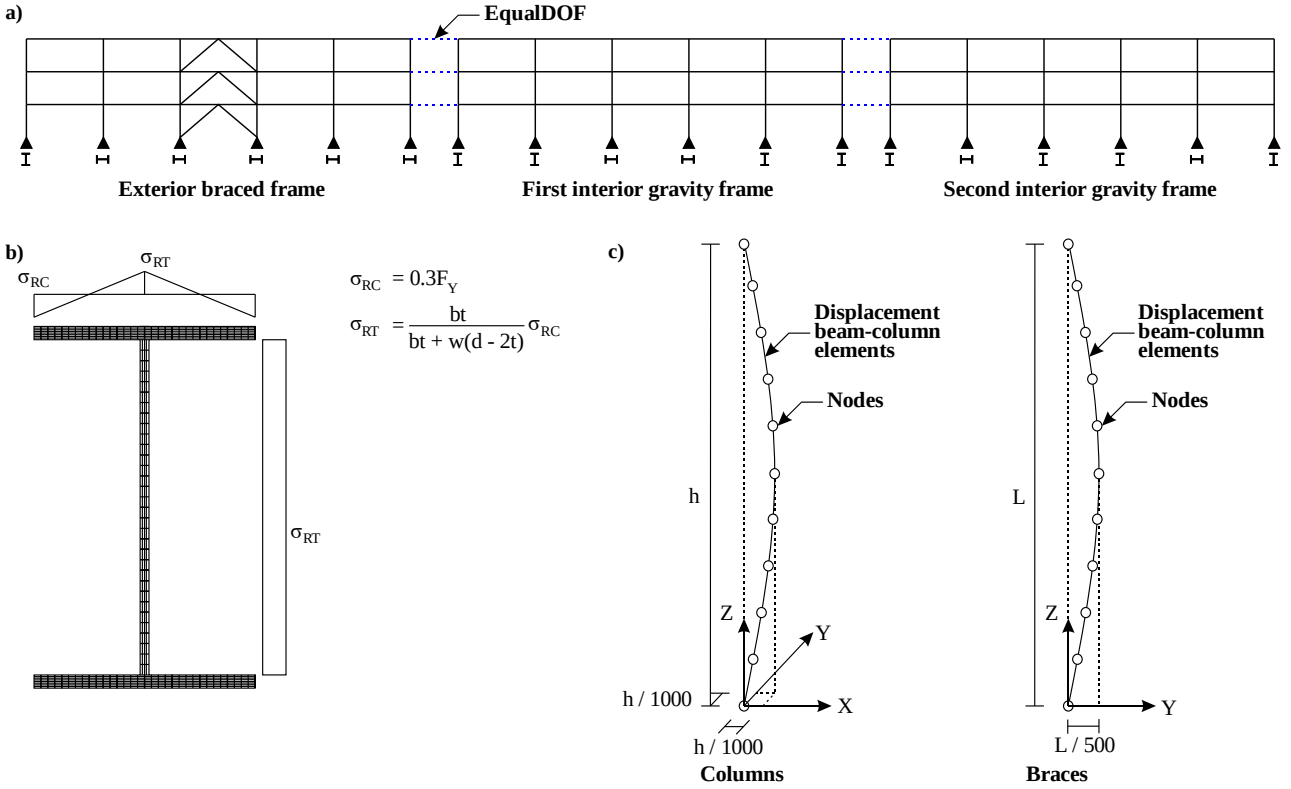

Fig. 2 – Building detailing: a) Prototype building modeling; b) Residual stress pattern in the columns [15]; c) Out-of-plumbness and element discretization of columns and braces.

All columns were modelled using displacement-based nonlinear beam-column elements with fiber discretization of the cross-section. The *Steel02* material, which can account for combined kinematic and isotropic hardening responses, was assigned to the cross-section fibers. The yield values stress was set equal to the probable yield stress R_yF_y specified in CSA S16 for the beams and columns (R_yF_y = 385 MPa) and for HSS sections (R_yF_y = 460 MPa). Column flanges were modelled with 5 fibers over the flange thickness, 10 fibers over the flange width, 5 fibers over the web thickness and 10 fibers over the web width. The flange width was discretized to account for the residual stresses in the section and because some columns are oriented for weak-axis bending in the plane of the frame. The residual stresses were assigned in the column fibers with the pattern proposed by Galambos and Ketter [15], presented in Fig. 2b.

The columns were discretized in 10 elements over their length to allow buckling response. Initial out-of-straightness was assigned in both orthogonal directions with a half-sine function having a maximum amplitude of h_s/1000, as shown in Fig. 2c. Column continuity was also considered in the numerical model. Each column was modelled with a pinned connection at the base. The beams of the braced frame were also modelled with displacement-based nonlinear beam-column elements to capture P-M interaction. The model was identical to that of the columns except that buckling out-of-plane was assumed to be prevented by the floor slab. Hence, out-of-straightness was included only in the vertical direction. The bracing members were also modelled using displacement-based nonlinear beam-column elements. For the braces, the probable yield stress was taken as 460 MPa, as specified by CSA S16. The braces were discretized in 10 elements and were assigned a half-sine out-of-straightness with L/500 amplitude in the out-of-plane direction, as pictured in Fig. 2c. The gravity beams were expected to deform elastically and were modelled with elastic-beam members.

2.3 Design and modelling of the PR beam-column connections

PR beam-column connections are introduced in the gravity frame to create moment-frames and ensure stable response for the structure in case of a brace connection failure during an earthquake. The connections must therefore possess sufficient rotational stiffness, strength and inelastic deformation capacity to achieve this behaviour. The minimum required stiffness is determined to obtain positive secant storey shear stiffness at any storey after removal of one brace in that storey, when considering P-Δ effects. The connections must also be capable of accommodating the rotation demand determined from spectral analysis of the structure with the missing brace. However, the connection flexural strength at this rotation must be limited to avoid creating plastic hinges in the gravity columns which were designed to support only gravity induced axial loads. The allowable maximum moment, either M_{fx} or M_{fy}, that can be resisted by the columns of the gravity frame in presence of the concomitant gravity loads can be determined using the compression-flexure interaction equation of required by CSA S16:

$$\frac{C_f}{C_r} + \frac{0.85 U_{1x} M_{fx}}{M_{rx}} + \frac{\beta U_{1y} M_{fy}}{M_{ry}} \leq 1.0 \quad (1)$$

In this expression, C_f is the compression load on the column due to 1.0D + 1.0E + 0.5L + 0.25S, C_r is the factored axial resistance of the member, M_{rx} and M_{ry} are the factored flexural resistances along the strong and weak axes, respectively, U_{1x} and U_{1y} are factors that account for moment gradient and P-δ effects, and β is an interaction coefficient. The top and seat angles of the PR connections of the prototype structure were designed to satisfy these requirements. Additional detail on connection design can be found in [13].

Force-displacement data from the experimental campaign on 139 individual angle specimens was used to quantify the influence of the angle thickness t and the column bolt position g_c on the cyclic response of bolted top and seat angles. A new *SteelAngles* uniaxial material, developed by Béland [13] and implemented in OpenSees to recreate the hysteretic behaviour of individual bolted angles, is then used to model the beam-column connection of the structure using a component-based approach. The *SteelAngles* material was created by modifying the existing *Steel02* material in OpenSees to implement mathematical expressions representing the various segments of the hysteretic response of angles as obtained from the test program on individual angles subjected to monotonic and cyclic inelastic demand [10]. A fatigue model is used in the model to reproduce strength degradation observed in large cycles. The input parameters of the model are determined from empirical expressions that involve geometrical parameters of the angles. Predicted and measured force-displacement responses for an individual L152x203x19.1 angle connected on the column flange with two 1" A490 bolts subjected to symmetrical cyclic test protocol with stepwise incremented amplitudes [10] are presented in Fig 3b. Fig. 3c compares the predicted and measured responses of the same angle under a real-time seismic induced displacement signal. As shown, excellent correlation can be obtained with the *SteelAngles* material for both loading conditions, including the strength degradation response exhibited by the specimen towards the end of the cyclic test.

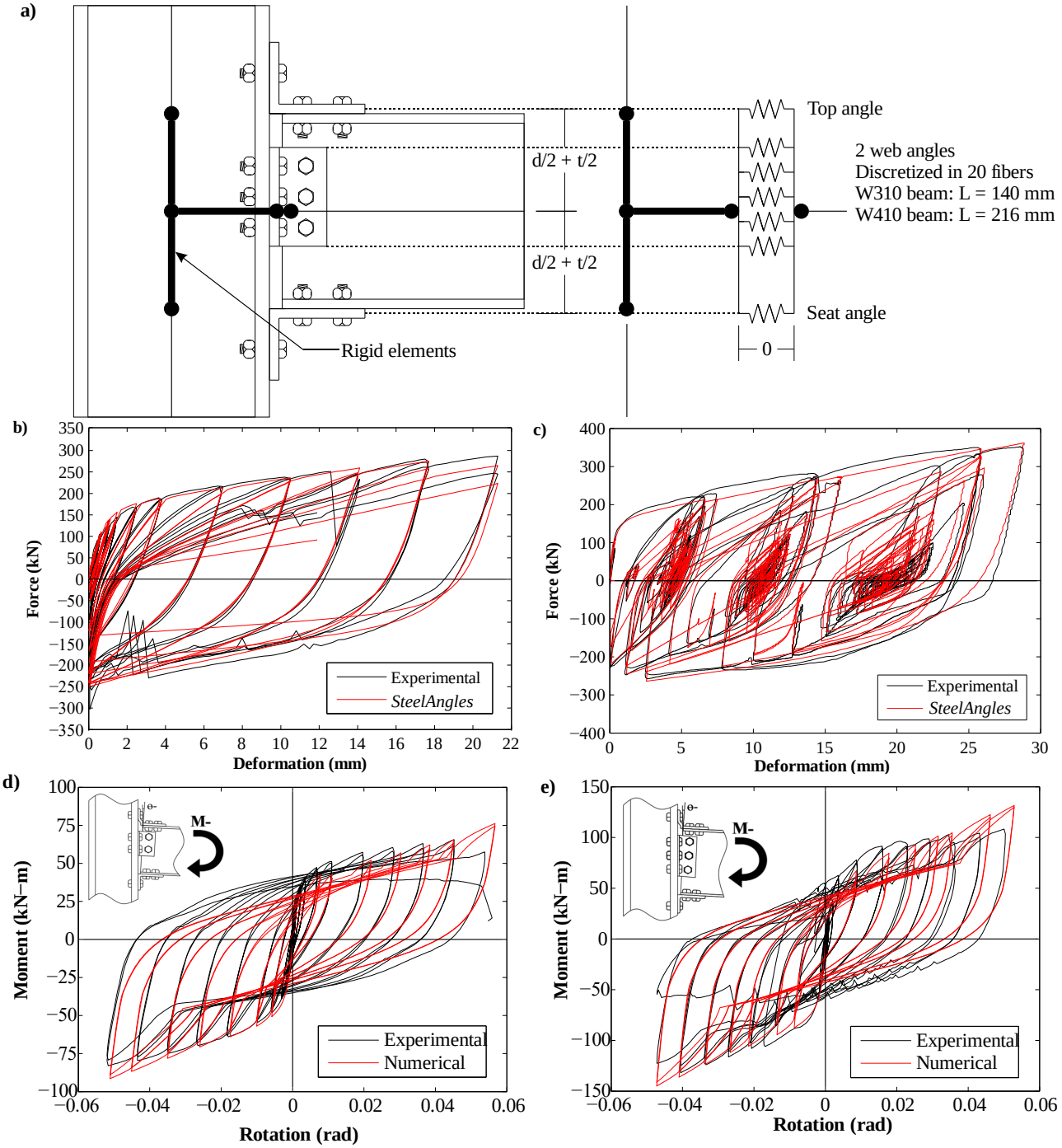

Fig. 3 – a) Numerical modeling of a typical gravity beam-column connection; b) and c) Measured and predicted hysteretic responses for an L152x203x19.1 angle [12] under cyclic (b) and seismic (c) loading; d) and e) Measured and predicted cyclic responses for W310 (d) and W410 (e) beam-column connections with web and top and seat angles.

In a beam-connection model with web and top and seat angles, the angles are modelled using fiber discretized *zerolengthSection* element with the *SteelAngles* material assigned to the fibers. For web angles in beam-column connections, the load in a given web angle fiber depends on its position along the height of the connection and relative distance to the neutral axis. These components were thus discretized into 20 fibers as shown in Fig. 3a. The values used for the input parameters of the web angle material model were defined for a unit width (b_{eff} = 1 mm). The area assigned to each fiber thus corresponds to the effective width of the

component. This material was modelled in parallel with a very stiff Elastic No-Tension (*ENT*) material [14] to represent the contact between the angle leg and the column flange. In a beam-column model, the top and seat angles are each represented by a single fiber, as shown in Fig. 3a, each fiber being assigned the *SteelAngles* material. In this case, the material properties of the top and seat angles are calculated using their total effective widths; therefore, the area of these fibers are set to 1.0. The top and seat angle material were also modelled in parallel with a stiff Elastic No-Tension (*ENT*) material to represent the contact between the angle column leg and the column flange.

The fiber section of the *zerolengthSection* is aggregated with a stiff material in its transverse direction, to avoid large vertical deformations. In a structure model, rigid elements are added between the column centerline and the column flange where the connection is located. The length of these rigid elements corresponds to half of the column depth and aims at modeling the connection on the flange of the column. However, the panel zone deformation of the column web is neglected with this modeling scheme.

Figs 3d and e compare numerical predictions with test results obtained from cyclic tests performed on two beam-column connections with web and top and seat angles during the experimental program on full-scale connections [12]. The numerical model generally shows a good agreement with the experimental results, although damage and degradation are not sufficiently considered in the numerical model. This shows that a simple component-based model can accurately represent the complex nonlinear behaviour of bolted angle connections. This connection model was then used in the complete building model.

As presented in Fig. 4, the gusset-beam-column connections in the building model were also created using the *zerolengthSection* element described previously. Fibers with web angle material are added to the section to represent the two angles attaching the gusset to the column flange. The brace element is modelled with a rigid element representing the gusset length. This rigid element is attached to the connection on the beam side, to transfer the brace load through the connection model.

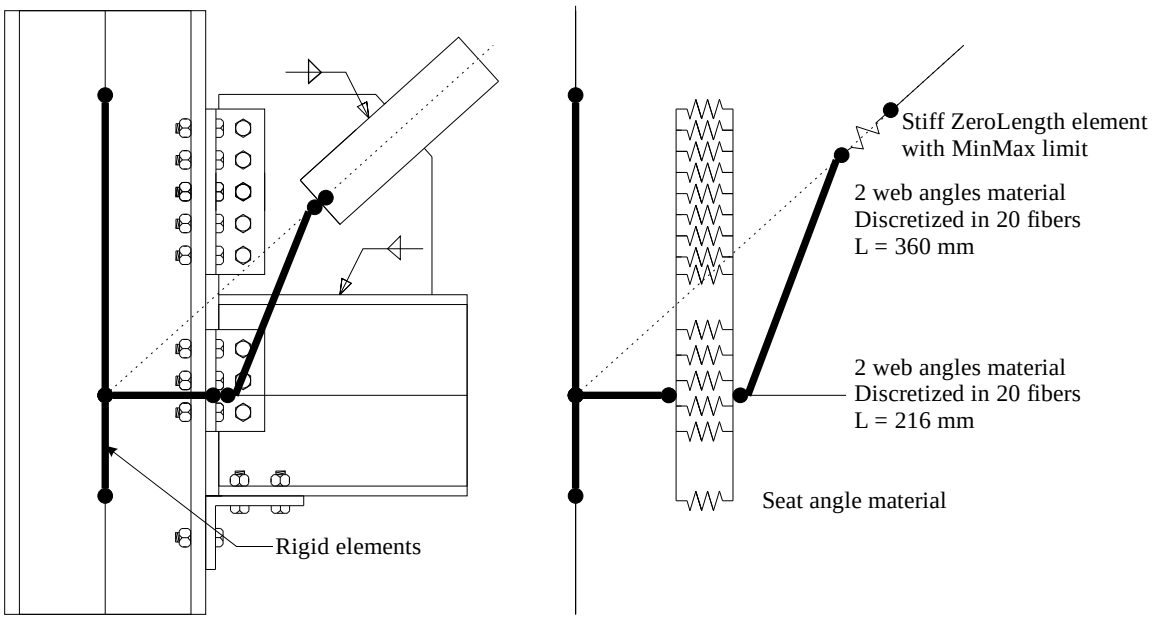

Fig. 4 – Numerical modeling of typical gusset-beam-column connections

The effective length of the brace corresponds to 90% of the centerline distance, which assumes a gusset plate length corresponding to 5% of the brace length at each end. Clause 27.11 of CSA S16-14 does not require ductile detailing for the gusset plates; the out-of-plane rotational behaviour of the gusset plates was therefore not included in the model. A field-welded slotted HSS connection was assumed for the braces. The welds between the gusset and the braces were modelled as *zerolength* elements [14] with a very stiff material in all 6 DOFs. The braces were thus considered fixed to the gusset plates. Brace connection failure in the analysis

was modelled by assigning a tensile and compressive force limits with a *MinMax* uniaxial material to the translational axial DOF of the connection *zerolength* elements. The *MinMax* uniaxial material force limit was set equal to 1.3 times the braced design compression force C_f to account for the connection overstrength which was taken equal to the overstrength-related factor R_o of the system. Once the limit is reached, the *zerolength* element is removed from the model, thus disconnecting the brace to the gusset plate. At the first storey of the structure model, the limit of the *MinMax* material was set equal to 1802 kN.

2.4 Seismic analysis

In the analysis, gravity loads corresponding to D+0.5L+0.25S were applied to the structure prior to performing the modal analysis and applying the seismic ground motions. Columns, braces, and beams were assigned co-rotational geometric transformation to account for P-delta effects in the analyses. Rayleigh damping was used in the time history analyses assuming 2% of critical in the first two modes of the structure. Tangent stiffness was considered in the damping model to account for the drop in brace axial stiffness and lengthening of the structure periods after brace connection failure. The structure models were then subjected to an ensemble of site representative ground motions scaled to match the design spectrum for a class C (firm ground) site C in Montreal.

3. Building response

The computed periods of the undamaged structure in the three translational modes, including P-delta effects, for the two models are presented in Table 2. Implementing the enhanced connections in the gravity frame of the building modified the building periods. However, these changes are small and likely have a no significant impact on the dynamic response of the buildings. The braced frame lateral stiffness is very large compared to that supplied by the gravity frame beam-column connections, so the behaviour of the building before brace connection failure is controlled by the braced frames.

Table 2 – Vibration periods of the undamaged two models including P-delta effects.

Period (s)	Pinned connections	Enhanced connections
T_1	0.686	0.680
T_2	0.289	0.309
T_3	0.201	0.217

The hysteretic responses of the braces in the building first storey as obtained under ground motion MC9 with the models with pinned and enhanced gravity connections are presented in Fig. 5a and b respectively. Under that MC9 ground motion, the two models exhibited a similar generally elastic behaviour. However, in Fig. 5b, the model with the enhanced connections showed a change in response in the cycle after reaching point A. This behaviour is attributed to yielding of the angles in the gusset-beam-column connection at the second storey which is indicated in Fig. 6a. In this connection, yielding of the uppermost fibers of the angles attaching the gusset plate to the column are located at a large distance from the beam centerline, which resulted to yielding under small rotations. In the model with pinned connections, the beams in the braced frame are also pin-connected and this behaviour was therefore not observed. In both models, brace connection failure occurred in the right-hand side (RHS) brace at compression forces of 1799 kN and 1814 kN for the models with pinned and enhanced connections, respectively. Occurrence of brace connection failure is indicated by point B in Figs. 5a and b.

After connection failure in the RHS brace, the LHS brace remained active but its effectiveness decreased significantly because the vertical support at the beam mid-span provided by the RHS brace was lost as shown in Fig. 6b. The brace frame lateral stiffness in the first storey was then reduced to the value governed by the flexural stiffness of the beam, similar to that of single-diagonal eccentrically braced frame (EBF) with long links (long link EBF mechanism) illustrated in Fig. 6c. For the structure studied, the storey

shear stiffness in the first-storey reduced from 218 kN/mm before connection failure to 4.88 kN/mm after connection failure. This residual lateral stiffness can be observed in Fig. 5b. Since the brace connections at the beam mid-span were pinned in the pinned building, this behaviour is not observed on Fig. 5a. This behaviour of the fractured brace frame is specific to the chevron brace configuration.

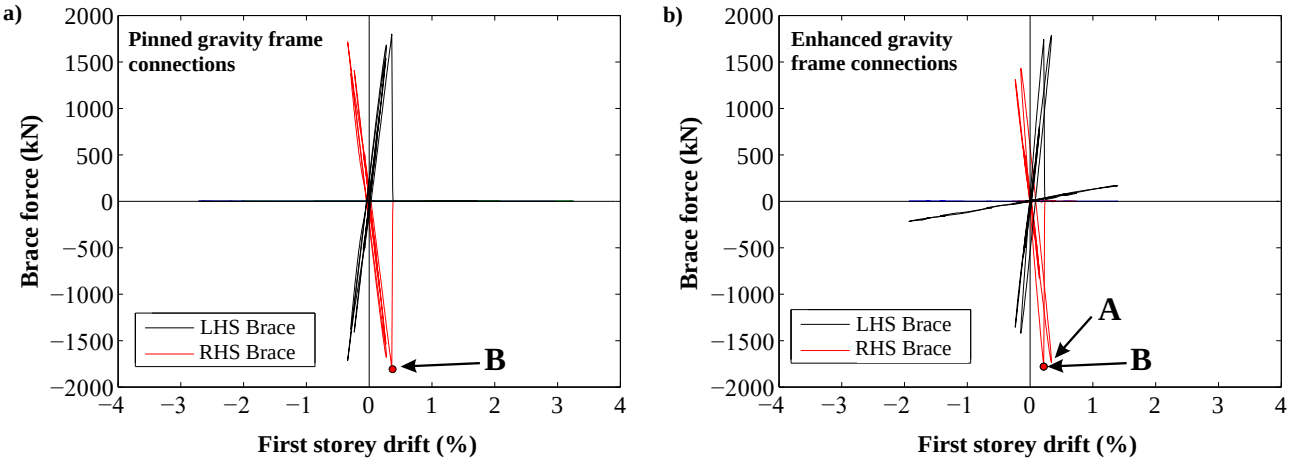

Fig. 5 – Hysteretic brace forces in the first storey under GM9 with the: a) Pinned connection model; b) Enhanced connection model.

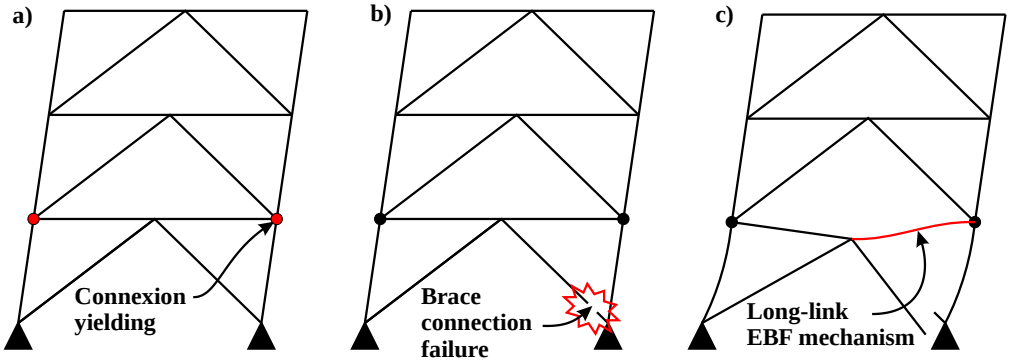

Fig. 6 – Braced frame deformation: a) at Point A; b) at Point B; and c) under lateral deformations developing after brace connection failure.

The variation of the base shear under the MC9 ground motion is presented in Fig. 7a for the two building models. Both models predicted similar response during the first cycles. Failure of the RHS brace connection occurred earlier in the building with the enhanced gravity frame connections. This difference is attributed to the fact that the structure with enhanced connections had higher lateral stiffness and attracted large inertia loads in the elastic range. After the brace connection failure, the base shear decreased drastically in both models. The storey drift in the first storey is given in Fig. 7b for each structure model. The reserve capacity provided by the enhanced gravity frame connections mitigated significantly the storey drifts, with a peak storey drift after brace connection equal to 1.93% of h_s. This value is less than the NBC limit of 2.5% h_s for buildings of the ordinary risk category. Conversely, the building with pinned gravity frame connections experienced much larger storey drifts, reaching up to 3.3% of h_s.

The bending moment in the interior gravity column C-2, at the upper end of the first storey, is presented in Fig. 7c. During the first few cycles before brace connection failure, the moment that developed in the column remained small for both structure models. However, after connection failure, the flexural capacity of the column is mobilized as larger storey drifts develop in the first storey. For the building with

pinned gravity frame connections, the peak moment 262 kN-m, which is significantly larger than the moment of 178 kN-m causing yielding of the column section in th presence of the gravity loads, according to Eq. (1) using probable resistances. For this structure, the large column moment is caused by the continuity of the gravity columns and the difference in storey drifts in the first and second storeys, as shown in Fig. 8a. Under this ground motion the moment triggered a plastic hinge in the column, which contributed further to the large storey drifts observed in the first level.

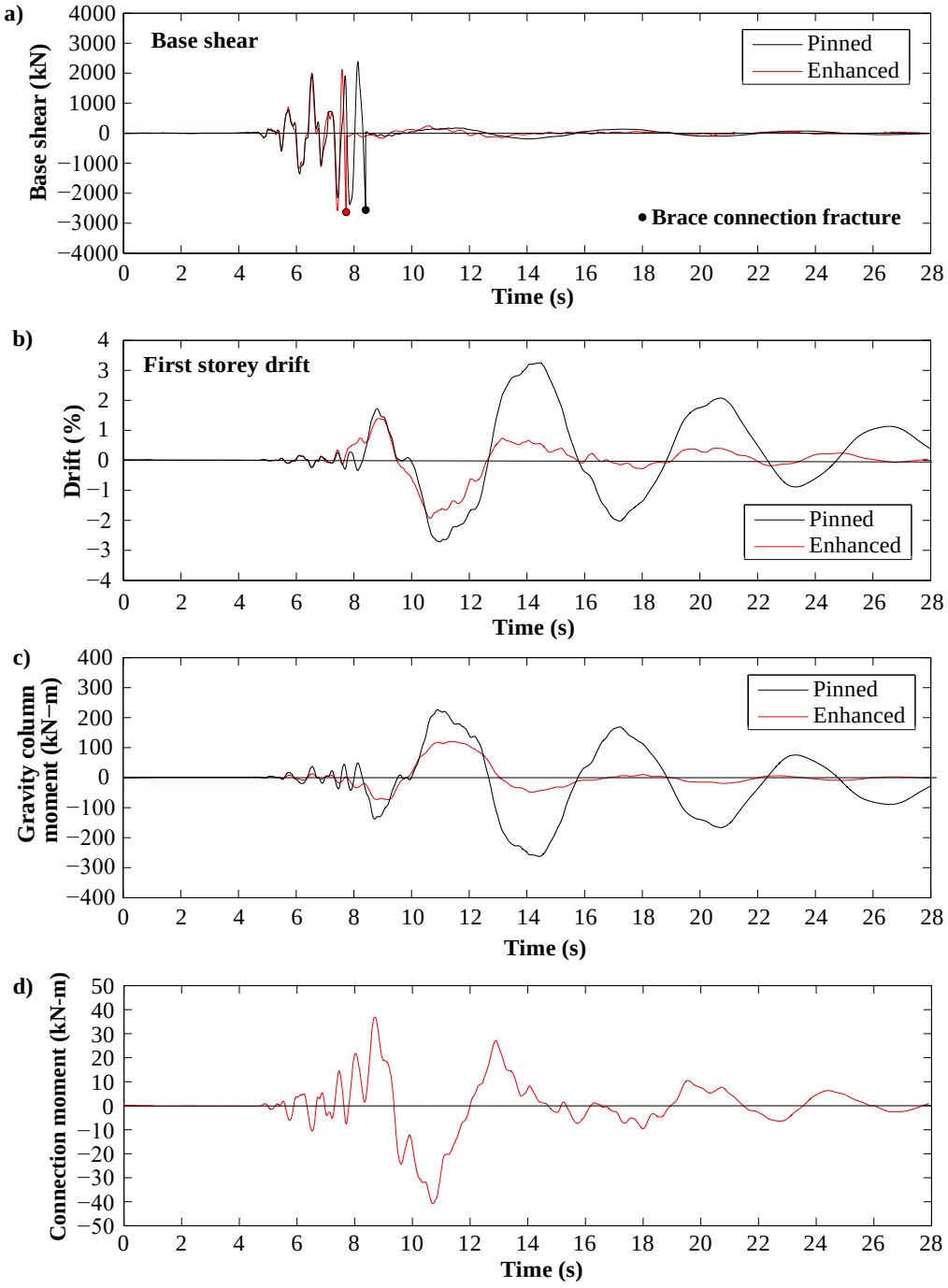

Fig. 7 – Time-history of the: a) Base shear; b) first storey drift; c) Moment in gravity column C-2 at the upper end of the first storey; d) Moment in the first-storey beam PR connection to column C-2.

Conversely, for the building with enhanced gravity frame connections, the maximum moment in the column (134 kN-m) remained within the capacity of the section and the column remained elastic. In this structure, column moments are also due to the difference in drifts between levels 1 and 2 but that difference is significantly less than in the building with pinned gravity frame connections. The moments are therefore mostly generated by the moment-frame action due to the enhanced PR connections (Fig. 8a). In that case, as a result of the design procedure, column moments induced by the beams are bounded by the capacity of the PR connections, and maximum moments remained within the limits adopted in design. Fig. 8b shows the moment-rotation response in the beam-column connection for the interior column examined.

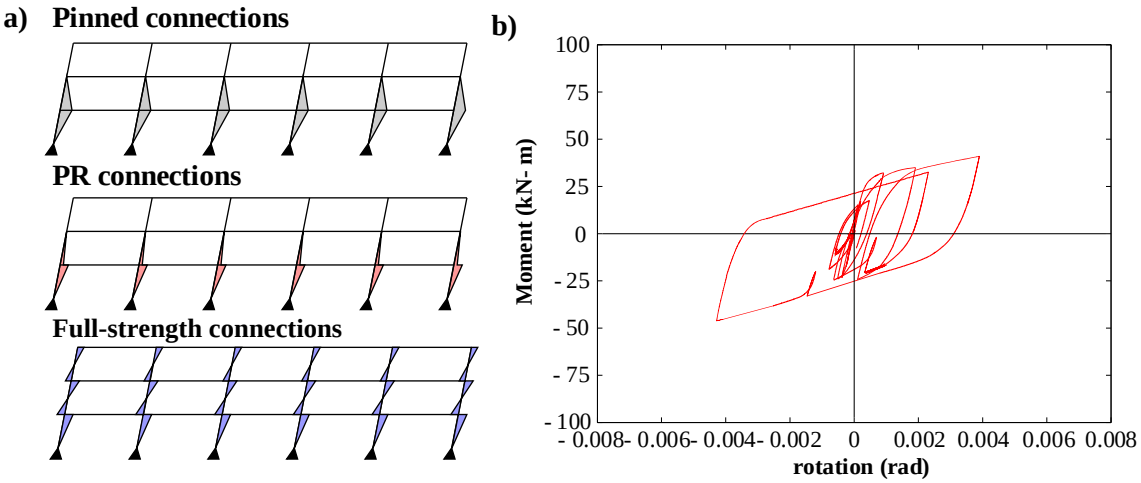

Fig. 8 – a) Schematic moment distribution in the gravity frame columns for various connection types; b) Hysteretic response of the first-storey beam PR connection to column C-2 under MC9 ground motion.

The history of the moment in the first-storey beam PR connection to column C-2 under ground motion MC9 is presented in Fig. 7d. The hystertic response of that connection is presented in Fig 8b. As expected, the connection did not experience significant rotational demand at the beginning of the earthquake and it remained essentially elastic with a maximum moment of approximately 20 kN-m. The connection was however mobilized after brace connection failure occurred. The connection then reached a maximum moment of 42 kN-m and exhibited a nonlinear ductile behaviour as intended by design. As shown in Fig. 8b, the maximum rotation experienced by the connection was equal to 0.004 rad, which satisfies the design limit.

In Fig 7, it is noted that the structure fundamental period lengthened significantly after failure of the brace connection in the first storey brace. This change in dynamic behaviour results in a reduced number of large displacement cycles being imposed to the structure, which represents another advantage of the reserve capacity concept as the inelastic deformation capacity of the PR connections is mobilized only for a few cycles, thereby reducing the likelihood of strength or stiffness degradation due to damage accumulation.

4. Conclusion

A detailed numerical model for bolted beam-column connection with bolted double web angles plus top and seat angles was developed in OpenSees using a component-based approach. This model employs a uniaxial material model that was also developed to reproduce the load-displacement response of individual angles subjected to cyclic inelastic loading. The two models have been validated against experimental results from single angle tests and full-scale beam-column connection tests. A numerical simulation was conducted to illustrate the potential for enhancing the collapse performance of low-ductility braced steel frames by using partially-restrained beam-column connections in the gravity framing system of a 3-storey building structure. The reserve capacity created by these gravity frame connections contributed to maintaining the seismic response within acceptable limits after failure of a first-storey brace connection. Compared to a building with pinned gravity frame connections, storey drifts and column moments were reduced, confirming the potential

for PR connections to decrease the risk of soft storey response and structural collapse. Additional numerical simulations of low-ductility braced frames with reserve capacity should be performed to further validate the concept and refine the proposed design procedure. Future studies should also incorporate more realistic representations of the rotational restraint offered by the column base plates in the first storey. Panel zone deformations in the PR beam-column should also be accounted for. Future studies should investigate the benefits of reserve capacity for braced frame with an X-bracing configuration.

5. Acknowledgements

This study was partially supported by the U.S. National Science Foundation (Grant No. CMMI-1207976), the American Institute of Steel Construction, the Natural Sciences and Engineering Research Council of Canada and the Fond de recherche du Québec, nature et technologies. The opinions and conclusions in this paper are those of the authors and do not necessarily reflect the views of those acknowledged here.

6. References

[1] NRCC (2015): *National Building Code of Canada, 14th ed.*, National Research Council of Canada, Ottawa, ON, Canada.

[2] ASCE (2016): *ASCE/SEI 7-16, Minimum Design Loads and Associated Criteria for Buildings and Other Structures*, American Society of Civil Engineers (ASCE), Reston, VI.

[3] CSA (2014): *CSA S16-14, Design of Steel Structures*, Canadian Standards Association, Toronto, ON, Canada.

[4] Hines EM, Appel ME, Cheever PJ (2009): Collapse performance of low-ductility chevron braced steel frames in moderate seismic regions. *Engineering Journal, AISC*, **46**: 149-180.

[5] Li G, Fahnestock LA (2013): Seismic Response of Single-Degree-of-Freedom Systems Representing Low-Ductility Steel Concentrically Braced Frames with Reserve Capacity. *Journal of Structural Engineering, ASCE*, **139**(2): 199-211.

[6] Flores FX, Charney FA, Lopez-Garcia D (2014): Influence of the gravity framing system on the collapse performance of special steel moment frames. *Journal of Constructional Steel Research*, **101**: 351-362.

[7] Azizinamini A (1985): *Cyclic characteristics of bolted semi-rigid steel beam to column connections*, Ph.D, College of Engineering, University of South Carolina, Columbia, SC, USA.

[8] Kishi N, Chen WF (1990): Moment-rotation relations of semirigid connections with angles. *Journal of Structural Engineering-ASCE*,**116**: 1813-1834.

[9] Abdalla KM, Drosopoulos GA, Stavroulaki GE (2014): Failure Behavior of a Top and Seat Angle Bolted Steel Connection with Double Web Angles. *ASCE Journal of Structural Engineering*, **141**(7): 04014172.

[10] Beland T, Bradley CR, Nelson J, Sizemore JG, Davaran A, Hines EM, Fahnestock LA, Tremblay R. (2020): Experimental parametric characterization of bolted angle connection behavior. *ASCE Journal of Structural Engineering*, DOI: 10.1061/(ASCE)ST.1943-541X.0002662.

[11] Beland T, Tremblay R, Hines EM, Fahnestock LA, (2020): Evaluating the rotational capacity of bolted double web angle beam-column gravity connections with full-scale experimental testing. *ASCE Journal of Structural Engineering*, DOI: 10.1061/(ASCE)ST.1943-541X.0002661.

[12] Beland T, Tremblay R, Hines EM, Fahnestock LA, (2020): Full-scale cyclic testing with shear load of double web with top and seat angle beam-column connections. *ASCE Journal of Structural Engineering. In review.*

[13] Beland T (2019): Improving the seismic robustness of conventional construction concentrically braced steel frames by mobilizing the gravity load framing system, Ph.D, Ecole Polytechnique de Montreal, Montreal, QC, Canada

[14] Mazzoni S, McKenna F, Scott MH, Fenves GL (2006): *OpenSees Command Language Manual*. University of California Berkeley: Pacific Earthquake Engineering Research Center, Berkeley, USA.

[15] Galambos TV, Ketter RL (1958): Columns under combined bending and thrust. *Journal of the Engineering Mechanics Division*, ASCE, **85**(2), 135-152.

